RevMexAA (Serie de Conferencias), **12**, 62–69 (2002)

THE ELECTRON TEMPERATURE IN IONIZED NEBULAE

Grażyna Stasińska

DAEC, Observatoire de Meudon, France

RESUMEN

Discutimos el papel que juega la temperatura electrónica en la determinación de abundancias en nebulosas planetarias y regiones H II gigantes. Mostramos que, aun cuando las observaciones permiten una estimación directa de T_e, las abundancias pueden tener errores significativos por razones diferentes a fluctuaciones en la temperatura o correcciones a la ionización y mostramos ejemplos de alta y baja metalicidad. Por otro lado, en ciertas circunstancias y aun cuando no exista una medida directa de T_e, se pueden dar estimaciones aproximadas (o límites) de las abundancias en GHRs y PNe. Enfatizamos que, a pesar que los mecanismos que definen a la temperatura electrónica en nebulosas ionizadas se conocen desde hace medio siglo, todavía existen problemas importantes por resolver. Finalmente, favorecemos una descripción de las inhomogeneidades en la temperatura diferente a la comunmente usada.

ABSTRACT

We discuss the role of the electron temperature in abundance determinations in ionized nebulae (planetary nebulae and giant H II regions). We show that, even when observations provide a direct estimate of T_e, abundance determinations may sometimes be significantly in error for reasons other than hypothetical temperature fluctuations or uncertainties in ionization correction factors, and we show striking examples both in the high and the low metallicity regimes. On the other hand, even without a direct measure of T_e and under certain conditions, it is possible to give rough estimates (or limits) on the abundances, both in GHRs and in PNe. Although the main mechanisms determining the electron temperature in ionized nebulae have been known for half a century, we emphasize that there are still important problems to be solved. Finally, we advocate for a different description of temperature inhomogeneities than the scheme generally used.

Key Words: **H II REGIONS — ISM: ABUNDANCES — PLANETARY NEBULAE**

1. INTRODUCTION

Emission lines, and especially the forbidden lines used for abundance determinations in ionized nebulae are strongly sensitive to the electron temperature, T_e. It is common thought that, when T_e can be derived directly from observed spectra, for example using the [O III] $\lambda4363/5007$ ratio, abundance determinations are fairly reliable. We will show that this is not necessarily the case (§3). We will also discuss the reliability of abundance determinations when T_e is not measured directly, both in the case of planetary nebulae (PNe) and giant H II regions (GHRs) (§4). Then, we will address the question of whether temperatures observed in ionized nebulae are compatible with the predictions from photoionization models and we will touch upon the problem of temperature inhomogeneities (§5).

2. BASICS

As is known from general considerations on the thermal balance in ionized nebulae (Spitzer 1948; 1949; Spitzer & Savedoff 1950; Osterbrock 1989), the electron temperature results from a balance between energy gains and losses. It is easy to show that, schematically, the energy gains per unit volume per unit time in a photoionized nebula can be written as:

$$G = n_e^2\, \alpha_A(\mathrm{H}^0, T_e)\, \frac{3}{2}\bar{E},$$

where n_e is the electron density, $\alpha_A(\mathrm{H}^0, T)$ is the recombination coefficient of hydrogen, and $\bar{E}$ is the mean energy of the absorbed photoelectrons, which is roughly proportional to the effective temperature of the ionizing radiation field, $T^\star$. Energy losses are due to a variety of processes, emission of collisionally excited lines being the most important. In a two-level approximation and neglecting collisional deexcitation, they can be schematically written as:

$$L = \sum_{ijl} n_e n(X^{ij})\, \frac{\Omega_l}{\omega_l}\, T_e^{-0.5} \exp\left(-\chi_l/kT_e\right)\, h\nu_l,$$

where $n(X^{ij})$ is the number density of ion X^{ij}, and the index l refers to a specific line, Ω_l being the collision strength, and χ_l the excitation level.

Ionized Gaseous Nebulae (Mexico City, 21-24 November 2000)
Editors: William Henney, José Franco, Marco Martos, & Miriam Peña

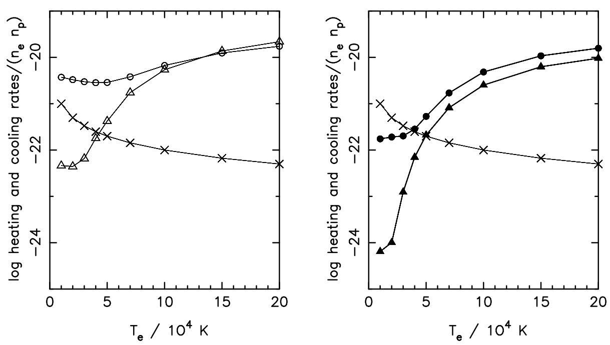

Fig. 1. Approximate heating and cooling rates divided by n_e^2, in arbitrary units. Circles: approximate cooling rates in the high excitation zone (O^{++} ions only). Triangles: cooling rates in the low excitation zones (O^+ and N^+ ions only). Left: $n_e = 100$ cm^{-3}; right: $n_e = 10\,000$ cm^{-3}. The heating rate is represented by crosses. By shifting the heating curve with respect to the cooling curves, one can understand how T_e varies with metallicity or with the effective temperature of the ionizing radiation field.

Thus, the electron temperature in a nebula is not a strong function of the distance to the ionizing stars, since it does not depend on the flux of ionizing photons. It is larger for higher values of $T^\star$ and lower values of the metallicity, Z. Figure 1 illustrates the heating and cooling rates in a photoionized nebula, at two different densities. At high density, the infrared fine-structure lines are partly quenched by collisional deexcitation, resulting in a larger T_e. Note also that, because of the shape of the cooling curves, there is a large temperature difference between the high and the low excitation zones at high metallicities.

3. WHEN T_e-BASED ABUNDANCE DETERMINATIONS ARE IN ERROR

3.1. *One Example at Low Metallicity: The Effect of Collisional Excitation of Hα*

At low metallicities, because of the high T_e, collisional excitation of the Hα line becomes non negligible and the Hα/Hβ ratio no longer has the recombination value. If the dereddening procedure of an observed spectrum involves Hα (which is commonly the case), this translates into an overestimation of the extinction $C(\mathrm{H}\beta)$, and an error in the dereddened line ratios. It can easily be shown that this error in the line ratios is *independent of extinction.* It can be large when the lines in question have very different wavelengths.

This is illustrated in Figure 2, which shows the results of photoionization models at metallicity $Z = 0.1 Z_\odot$ for evolutionary sequences of planetary nebu-

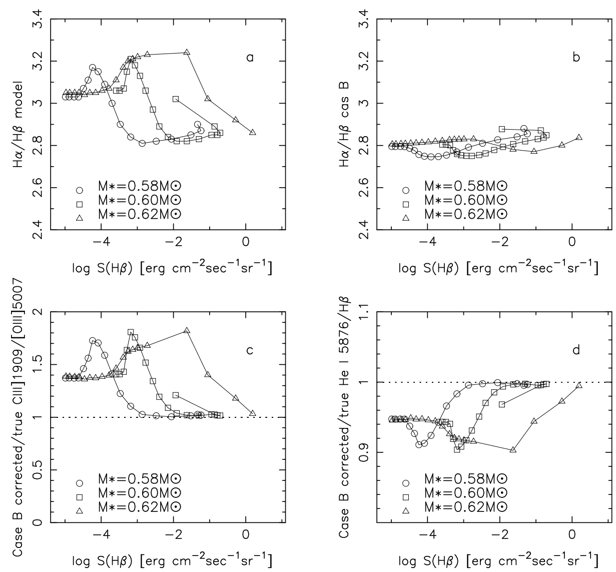

Fig. 2. Photoionization models for evolving PNe with $Z = 0.1 Z_\odot$, $M_{\rm neb} = 0.2 M_\odot$, $v_{\rm exp} = 20$ km s^{-1}. (a) computed Hα/Hβ; (b) case B Hα/Hβ; (c) C III] λ1909/[O III] λ5007 "dereddened" using case B with respect to actual C III] λ1909/[O III] λ5007; (d) same as (c) for He I λ5876/Hβ.

lae whose central stars follow the theoretical tracks of Blöcker (1995). These models were computed using the procedure outlined in Stasińska, Richer, & McCall (1998)[1]. We see that, at such a metallicity, there is quite a range in epochs during the evolution of PNe (materialized in the figure by the surface brightness in Hβ), where Hα/Hβ is significantly larger than the recombination value. The resulting error in the derived helium abundance may reach 5–10%. A similar effect is expected in very low metallicity H II regions. This is important to keep in mind for the determination of the pregalactic helium abundance from low metallicity GHRs. Davidson & Kinman (1985) indeed warned about this effect, but it does not seem to have been properly taken into account in later studies (see, e.g., Olive, Steigman, & Skillman 1997 or Izotov et al. 1999 and references therein). The error in C/O obtained using the C III] λ1909 and [O III] λ5007 lines may reach almost a factor 2 in the PN models shown here. Again, a similar effect is expected in low metallicity GHRs. This could explain why the carbon abundance estimated in I Zw 18 is larger than expected for its metallicity (Garnett et al 1997a). However, in the case of UV data, a possibly

[1]Unless otherwise stated, the photoionization calculations presented here used the code PHOTO as described by Stasińska & Leitherer (1996).

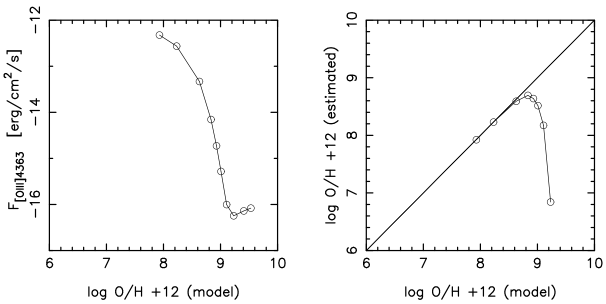

Fig. 3. Results from a simple model for a GHR having $T_* = 45\,000$ K, $Q_{\rm H} = 3\times10^{51}$ ph s^{-1}, $n = 30$ cm^{-3}, filling factor = 0.1. Left: predicted flux in the [O III] λ4363 line for an object at a distance of 1 Mpc; right: O/H derived by the classical $T_{\rm e}$-based method as a function of input O/H.

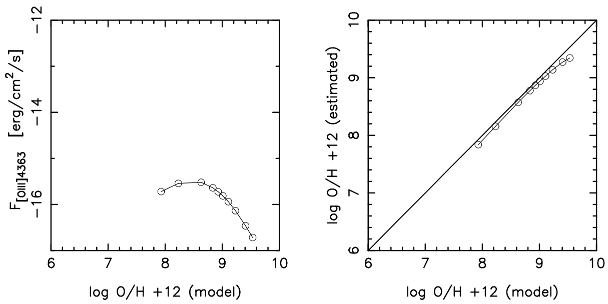

Fig. 4. Same as Fig. 3 for a simple model of an ionization bounded PN having $T_* = 150\,000$ K, $Q_{\rm H} = 3\times10^{47}$ ph s^{-1}, $n = 10^4$ cm^{-3}, filling factor = 0.3.

Ionized Gaseous Nebulae (Mexico City, 21-24 November 2000)
Editors: William Henney, José Franco, Marco Martos, & Miriam Peña

even more important problem is the uncertainty in the reddening law (Garnett et al 1999).

3.2. *One Example at High Metallicity: The Absence of [O III] Optical Lines from the O^{++} Zone*

At high Z, because of the intense cooling by the forbidden lines, $T_{\rm e}$ is low (see Fig. 1) and the transauroral lines used for $T_{\rm e}$ diagnostics become hard to detect. So far, there has been no $T_{\rm e}$-based measurement of metallicities higher than about 0.5 $Z_\odot$ in any GHR. With 8 m-class telescopes, however, it becomes possible to detect weak [O III] λ4363 fluxes, and the hope has been expressed that it will be possible to directly probe oxygen abundances at metallicities higher than solar. However, as already shown by Stasińska (1978) and Garnett (1992), high metallicities induce an important temperature drop in the O^{++} zone because cooling is dominated by the [O III] 52 μm and [O III] 88 μm lines which are almost independent of $T_{\rm e}$ (see Fig. 1). Therefore, the value of $T_{\rm e}$ derived from [O III] λ4363/5007 would largely overestimate the temperature characteristic of the O^{++} zone. Consequently, classical $T_{\rm e}$-based methods would strongly underestimate the oxygen abundance. This is illustrated in Figure 3. The derived O/H ratio always stays below the solar value, and would be underestimated by orders of magnitudes for metallicities over twice solar if such methods were applied. Incidentally, note the rise in the [O III] λ4363 flux at $\log {\rm O/H} + 12 > 9.1$. This is due to the fact that recombination becomes the dominant process for the excitation of this line at the low temperatures involved.

Does this mean that it is impossible to reliably determine the oxygen abundance in the central parts of galaxies, where it is supposed to be oversolar? The most straightforward way, of course, would be to use the [O III] 52 μm line (Simpson et al. 1995, Rudolph et al. 1997). Another possibility, suggested by Stasińska (1980), would be through high spatial resolution emission line imaging. Metal rich GHRs would show very characteristic and unusual spatial correlations between line intensities, since [O III] and [O II] and would be emitted almost cospatially in the high $T_{\rm e}$ zones, while the hydrogen and helium recombination lines would preferentially arise in the low $T_{\rm e}$ zones. Of course, detailed photoionization modeling reproducing the observed tendencies would still be necessary to provide a quantitative estimate of O/H.

Planetary nebulae provide an interesting substitute to GHRs for abundance determinations in the central parts of galaxies. As shown by Richer, McCall, & Stasińska (1998), the most luminous PNe are good tracers of the ISM oxygen abundance. Such PNe, being young (therefore dense) and excited by stars with $T^\star$ of the order of 100 000 K, have larger $T_{\rm e}$ than GHRs of same metallicity (see Fig. 1). Therefore, they can be detected in [O III] λ4363, even though their intrinsic luminosity is orders of magnitudes smaller than that of GHRs (compare Figs. 4 and 3). In addition, electron temperature gradients are not expected to be so severe as in GHRs (as can be seen from Fig. 1), so that the classical $T_{\rm e}$-based method to derive O/H should give reasonable results. Indeed, Figure 4 shows that, at least theoretically, this is the case.

4. ESTIMATING O/H WITHOUT $T_{\rm e}$

4.1. *Strong Line Methods for GHRs and PNe*

It has been shown by Pagel et al. (1979) that, in GHRs, provided that the hardness of the ionizing radiation field is related to the metallicity, it should be possible to calibrate some well chosen strong line ratios as a function of O/H (see Stasińska 2001 for a summary of the basics and a short bibliography of

Ionized Gaseous Nebulae (Mexico City, 21-24 November 2000)
Editors: William Henney, José Franco, Marco Martos, & Miriam Peña

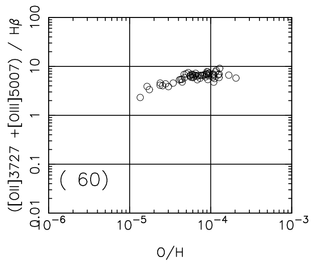

Fig. 5. ([O III] λ5007 + [O II] λ3727) / Hβ versus O/H for GHRs in a sample of blue compact galaxies with T_e-based derivations of O/H. Data from Izotov & Thuan (1999 and references therein). The number of objects is indicated in parenthesis.

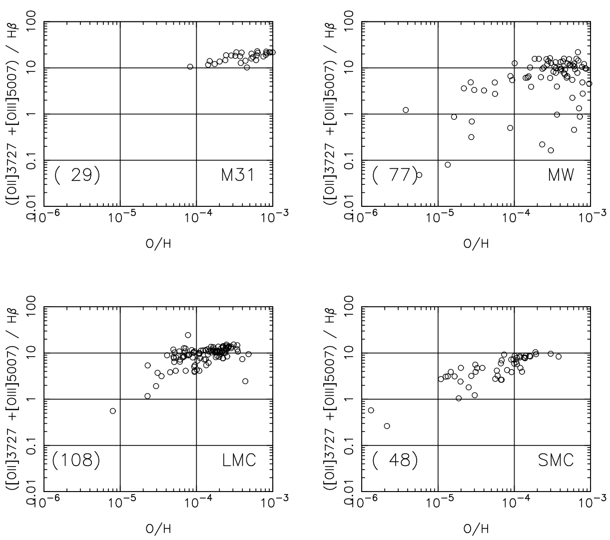

Fig. 6. Same as Fig. 5 for PNe in various galaxies: M31, the bulge of the Milky Way, the LMC and the SMC. Data as collected in Stasińska et al. (1998).

strong line methods). The extremely tight correlation between ([O III] λ5007 + [O II] λ3727) / Hβ and T_e-based O/H determinations in high signal-to-noise observations of H II galaxies (see Fig. 5) is an empirical confirmation that this method works at low metallicities, as was suggested by Skillman (1989). Incidentally, this implies that GHRs in blue compact galaxies constitute a very homogeneous class as regards their excitation and nebular properties (see discussion in Stasińska, Schaerer, & Leitherer 2001).

Can such a strong line method be applied to PNe? Since PN central stars span a wide range in $T^\star$ (30 000–200 000 K), one does not expect such methods to work in the same way as for GHRs. However, Figure 6 shows that PNe outline a rather well defined

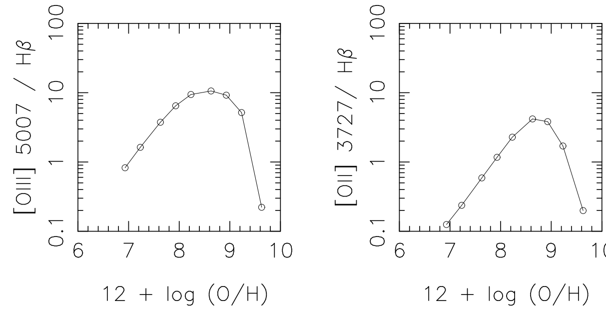

Fig. 7. Variation of [O III]/Hβ and [O II]/Hβ as a function of O/H for a simple density bounded model of PN with $M_{\rm neb} = 0.5 M_\odot$, $T_* = 100\,000$ K, $Q_{\rm H} = 3 \times 10^{47}$ ph s^{-1}, $n = 10^3$ cm^{-3}.

upper envelope in the ([O III] λ5007 + [O II] λ3727) / Hβ vs. O/H plane, as already noted by Richer (1993) for Magellanic Clouds PNe. This upper envelope probably corresponds to the hottest central stars, and can be used to infer a lower limit for O/H. Such a procedure has been used by Richer & Mc Call (1995) and Richer et al. (1998) for extragalactic PNe with [O III] λ4363 undetected.

4.2. *Photoionization Modeling*

Contrary to a widespread opinion, photoionization models (be it of PNe or of GHRs) are usually incapable of providing abundances if T_e is not directly measured. It is easy to produce models differing only in abundance ratios that will reproduce all the observed emission lines. This is illustrated in Figure 7, which shows the run of [O III]/Hβ and [O II]/Hβ as a function of O/H for a simple PN model. The reason of such a behavior is the same for PNe and GHRs and has been widely commented in the literature. As O/H increases, T_e decreases due to enhanced cooling, and the optical forbidden lines are gradually overtaken by the infrared lines, leading to these bell-shaped curves. The maximum of the curves occurs at a metallicity around solar for dense PNe ionized by stars with $T^\star > 100\,000$ K, and around half solar for GHRs.

Table 1 shows the results of photoionization modeling of the Galactic Bulge PN PNG 351.2+05.2 (M 2-5) for which Ratag (1991; 1997) had claimed an abundance of one fourth solar. Using the Lviv photoionization code, Stasińska, Malkov, & Golovaty (1995, unpublished) produced two classes of models for this object accounting satisfactorily for the observed data (line strengths, total flux and radius). The first one indeed has an oxygen abundance similar to Ratag's, but the second has O/H larger than solar!

TABLE 1

MODELS FOR THE PN M 2-5

	obs	Ratag	SMG low Z	SMG high Z
T_* (K)		37500	39000	39000
r_* (10^{10} cm)			5.0	4.9
$R_{\rm in}$ (pc)			0.062	0.065
$R_{\rm out}$ (pc)	0.10		0.087	0.085
$-\log F(\mathrm{H}\beta)$	11.409		11.407	11.411
n (cm^{-3})		2050	1800	1800
He		0.117	0.117	0.100
C			1.5×10^{-3}	1.2×10^{-3}
N		4.8×10^{-4}	2.5×10^{-4}	6.0×10^{-4}
O		2.2×10^{-4}	2.4×10^{-4}	1.2×10^{-3}
Ne			5.0×10^{-5}	2.4×10^{-4}
S		2.3×10^{-5}	3.0×10^{-6}	7.0×10^{-6}
O II 3727	0.596		0.587	0.604
Ne 3869			0.014	0.0096
O III 4363	<0.0013		0.0006	0.0001
He II 4686			0.0004	0.0003
H I 4861	1.00		1.00	1.00
O III 5007	0.283		0.304	0.275
N I 5200	0.0149		0.0043	0.0087
N II 5755	0.0071:		0.0151	0.0060
He I 5876	0.128		0.126	0.128
O I 6300			0.0054	0.0116
N II 6584	2.85		2.79	2.81
S II 6717	0.0565		0.053	0.0558
S II 6731	0.084		0.077	0.0826
O II 7325	0.0091:		0.0126	0.0063

This demonstrates that, in absence of a direct measure of $T_{\rm e}$, photoionization modeling by itself does not necessarily give a clear clue to the metallicity of nebulae when only optical data are available. In some cases, however, when solutions on either the low or high metallicity side can be rejected using arguments of astrophysical nature, photoionization modeling can provide estimates of O/H.

An example where photoionization modeling gives interesting limites on O/H is the recently discovered PN in the Galactic halo, SBS 1150+599A (now PN G135.9+55.9, for full details see Tovmassian et al. 2001 and these proceedings). In that case, solutions at high metallicity can obviously be discarded. There is still a wide range of solutions compatible with the observed line ratios, but when additional considerations are taken into account, it is found that the object has O/H of the order 1/500 solar (making it possibly the most oxygen-poor object known in the Galaxy).

5. DO WE UNDERSTAND THE TEMPERATURE IN IONIZED NEBULAE?

So far, we have not questioned the electron temperature itself. As a matter of fact, there are indications that simple photoionization models are incapable of reproducing satisfactorily the observed $T_{\rm e}$ in quite a variety of situations. There are cases of GHRs as well as of PNe, where photoionization models give too low a $T_{\rm e}$ (Campbell 1990; García-Vargas et al. 1997; Stasińska & Schaerer 1999; Luridiana et al. 1999; Luridiana & Peimbert 2001; Peña et al 1998), calling for additional heating sources. In other cases, however, no T_e problem is apparent (González Delgado & Pérez 2000) and in some cases, models seem to give too high a T_e (Oey et al. 2000). So far, we are still lacking a synthetic view of these anomalies. One difficulty is that, even if a model reproduces the observed line ratios satisfactorily, this does not necessarily mean that the model is a fair representation of the object. For example, the first attempts to solve the T_e problem in I Zw 18 were not supported by later observations (see discussion in Stasińska & Schaerer 1999).

It is of prime importance to understand what determines T_e in real nebulae if one wishes to derive reliable abundances, since one way or another, the observed line ratios used to derive abundances from optical or ultraviolet data depend on T_e.

In the following, we comment on two disputed topics.

5.1. *Temperature Gradients in Photoionized Nebulae*

While the electron temperature, being determined by the hardness of the ionizing photons and not on their flux (cf. § 1), does not necessarily fall off with radius, some T_e gradients are nevertheless expected. A consideration of the heating and cooling curves (Fig. 1) shows that T_e should rise outwards if the outer zones contain ions that are less efficient for the cooling. As mentioned above, the effect can be quite strong at metallicity above solar. At low metallicity, on the other hand, T_e decreases outwards. The hardening of the absorbed photons towards the ionization front, due to the frequency dependence of the photoabsorption cross-section is another factor that affects the radial T_e distribution. The predicted effect is however rather mild (see, e.g., the GHRs models of Stasińska & Leitherer 1996, or the grid of PN models from Stasińska et al. 1998).

Temperature gradients can be estimated from the comparison of T_e derived from various line ratios, such as [O III] $\lambda4363/5007$ and [N II] $\lambda5755/6584$ (see, e.g., Garnett et al. 1997b for GHRs and McKenna et al. 1996; Kingsburgh & Barlow 1994 for PNe). Recently, Peña, Stasińska, & Medina (2001) found that in PNe with Wolf-Rayet central stars, T_e([O III])/T_e([N II]) could be significantly different from 1 (by as much as 40%) and that it seemed to decrease with increasing O^{++}/O^{+}. Such a tendency cannot be reproduced by classical photoionization models. Dopita & Sutherland (2000) have shown that, by including the photoelectric effect on dust grains, one obtains larger T_e gradients than in dust free models, because dust heating affects essentially the inner zones. The cases with T_e([O III])/T_e([N II]) $\ll 1$ observed by Peña et al. (2001) however remain unexplained. One possibility is to advocate a contribution from shock heating in the outer zones, but quantitative models have still to be worked out.

5.2. *Temperature Inhomogeneities*

In a seminal paper, temperature inhomogeneities have been advocated by Peimbert (1967) to explain the discrepancies between T_e as determined by various methods. Peimbert introduced the temperature fluctuation scheme and observational work accumulated over the years by Silvia Torres-Peimbert, Manuel Peimbert and their coworkers and disciples seems to indicate a value of $t^2 \sim 0.04$. There are many questions about the reality, the ubiquity and the causes of these T_e fluctuations (see e.g., papers by Esteban, Peimbert, Binette, Liu and Péquignot in this volume, and references therein).

In fact, the temperature fluctuation scheme may not be quite appropriate to describe temperature inhomogeneities in ionized nebulae. A different approach was presented by Mathis et al. (1998). Here, and in order to help visualizing the problem, we use a toy model consisting of two homogeneous zones of volumes V_1 and V_2 with temperatures T_1 and T_2, electron densities n_1 and n_2, and densities of the emitting ions (e.g., O^{++}) N_1 and N_2. If we call f the ratio $(N_2n_2V_2)/(N_1n_1V_1)$ of the weights of the emitting regions, the mean electron temperature defined by Peimbert (1967) becomes

$$T_0 = \frac{T_1 + fT_2}{1 + f},$$

and the fluctuation parameter becomes

$$t^2 = \frac{(T_1 - T_0)^2 + f(T_2 - T_0)^2}{(1 + f)T_0^2}.$$

In Figure 8 (resp. 9) we explore the values of f that lead to the canonical value $t^2 = 0.04$ at $T_0 = 8000$ K (resp. $T_0 = 15\,000$ K), and show the effect on the O^{++} abundances calculated by using the T_e derived from [O III] $\lambda4363/5007$. The case $f = 1$, i.e., regions of equal weight, corresponds to $T_1 = 12\,000$ K and $T_2 = 8000$ K. This is quite a large temperature difference, which would correspond to heating- or cooling rates differing by about a factor 3 between the two zones (see Fig. 1). No wonder that photoionization models have difficulties in producing such values of t^2 around these temperatures! When $f \gg 1$, there is a high weight zone at $T_2 \leq T_0$ and a low weight zone at $T_1 \gg T_0$. Such a situation could

Ionized Gaseous Nebulae (Mexico City, 21-24 November 2000)
Editors: William Henney, José Franco, Marco Martos, & Miriam Peña

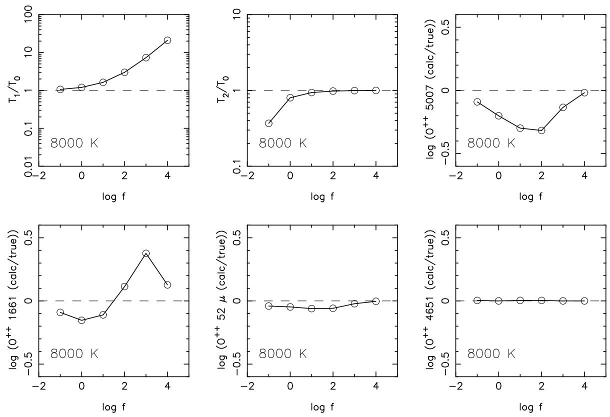

Fig. 8. Results from a two zone toy model defined by T_0=8 000 K and $t^2 = 0.04$ (see text).

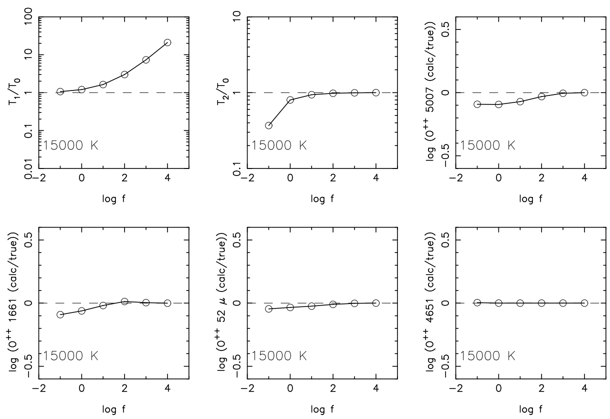

Fig. 9. Results from a two zone toy model defined by T_0=15 000 K and $t^2 = 0.04$ (see text).

correspond to a photoionized nebula with small regions being heated by shocks or conduction. When $f \ll 1$, there is a high weight zone at $T_1 \geq T_0$ and a low weight zone at $T_2 \ll T_0$ which could correspond to high metallicity clumps.

As expected, Figures 8 and 9 show that the O^{++} derived from infrared fine structure lines is correct. The optical recombination line O II λ4651 also give a correct O^{++}. However, high temperature dielectronic recombinations are not included in the present day atomic calculations. They might well boost O II λ4651 in zones of high T_e (around 20 000–50 000 K, see Liu et al. 2000; Dinerstein et al. 2000). This is an attractive explanation for the fact that in PNe, O^{++} abundances derived from recombination lines are far greater than derived from optical or infrared lines (see Liu, these proceedings). Compared to the alternate explanation invoking oxygen-rich condensations (Liu et al. 2000, Péquignot, these proceedings), this one has the advantage of being naturally fulfilled if additional heating mechanisms substantially raise the electron temperature in limited volumes of the emitting gas, such as shock or conduction fronts. Besides, they do not require us to find a mechanism to produce oxygen-rich pockets in planetary nebulae.

Following expectations, O^{++} derived from [O III] λ5007 is generally underestimated, but it is interesting to note that the magnitude of the effect depends both f and on T_0. It is negligible when log $f > 3$–4, because [O III] λ4363 saturates above $\sim$ 50 000 K. In the T_0 = 15 000 K case, the effect is never strong anyway. For the T_0 = 8000 K case, errors in O^{++} of up to a factor 2–3 can occur in the regime where [O III] λ4363 is significantly emitted in both zones. As for O III] λ1661, it may lead either to an underestimation or to an overestimation of O^{++}/H, because the dynamical range of the line is larger than that of [O III] λ4363.

Figures 8 and 9 thus amply demonstrate that the classical temperature fluctuation scheme can be misleading. Even in a simple two zone model, the situation needs 3 parameters to be described, not 2. In our representation, these parameters would be T_1, T_2 and f, but other definitions can be used. This means that care must be taken when drawing conclusions on temperature inhomogeneities by comparing abundances derived from various lines. We argue that such diagrams as shown here might be useful to pinpoint the physical cause of temperature inhomogeneities in ionized nebulae.

This wandering—and wondering—about the electron temperature in ionized nebulae is dedicated to Silvia Torres-Peimbert and Manuel Peimbert, at the occasion of a meeting in their honor. I am grateful to the Organizing Committee for having made my participation in this stirring conference possible.

REFERENCES

Blöcker, T. 1995, A&A, 299, 755
Campbell, A. 1990, ApJ, 362, 100
Davidson, K., & Kinman, T. D. 1985, ApJS, 58, 321
Dinerstein, H. L., Lafon, C. E., & Garnett, D. R. 2000, in ASP Conference Series Vol. 199, Asymmetrical Planetary Nebulae II: From Origins to Microstructures, eds. J. H. Kastner, N. Soker, & S. Rappaport (San Francisco: ASP), 301
Dopita, M. A., & Sutherland, R. S. 2000, ApJ, 539, 742
García-Vargas, M. L., González Delgado, R., Pérez, E., Alloin, D., & Terlevich, E. 1997, ApJ, 478, 112

Garnett, D. R. 1992, AJ, 103, 1330
Garnett, D. R., Shields, G. A., Skillman, E. D., Sagan, S. P., & Dufour, R. J. 1997a, ApJ, 489, 63
Garnett, D. R., Skillman, E. D., Dufour, R. J., & Shields, G. A. 1997b, ApJ, 481, 174
Garnett, D. R., Shields, G. A., Peimbert, M., Torres-Peimbert, S., Skillman, E. D., Dufour, R. J., Terlevich, E., & Terlevich, R. J. 1999, ApJ, 513, 168
González Delgado, R. M., & Pérez, E. 2000, MNRAS 317, 64
Izotov, Y. I., & Thuan, T. X. 1999, ApJ, 511, 639
Izotov, Y. I., Chaffee, F. H., Foltz, C. B., Green, R. F., Guseva, N. G., & Thuan, T. X., 1999, ApJ, 527, 757
Kingsburgh, R. L., & Barlow, M. J. 1994, MNRAS, 271, 25
Liu, X.-W. 2002, RevMexAA(SC), 12, 70 (this volume)
Liu, X.-W, Storey, P. J., Barlow, M. J., Danziger, I. J., Cohen, M., & Bryce, M. 2000, MNRAS, 312, 585
Luridiana, V., & Peimbert, M. 2001, ApJ, 553, 663
Luridiana, V., Peimbert, M., & Leitherer, C. 1999, ApJ, 572, 110
McKenna, F. C., Keenan, F. P., Kaler, J. B., Wickstead, A. W., Bell, K. L., & Aggarwal, K. M. 1996, PASP, 108, 610
Mathis, J. S., Torres-Peimbert, S., & Peimbert, M. 1998, ApJ, 495, 328
Oey, M. S., Dopita, M., A., Shields, J. C., & Smith, R. C. 2000, ApJS, 128, 511
Olive, K. A., Steigman, G., & Skillman, E. D. 1997, ApJ 483, 788
Osterbrock, D. E. 1989, Astrophysics of Gaseous Nebulae and Active Galactic Nuclei (Mill Valley, CA: USB)
Pagel B. E. J., Edmunds M. G., Blackwell D. E. et al. 1979, MNRAS, 189, 95
Peimbert, M. 1967, ApJ, 150, 825
Peña, M., Stasińska, G., Esteban, C., Koesterke, L., Medina, S., & Kingsburgh, R. 1998, A&A, 337, 866
Peña, M., Stasińska, G., & Medina, S. 2001, A&A, 367, 983
Péquignot, D. P. 2002, RevMexAA(SC), 12, 142 (this volume)
Ratag, M. A. 1991, thesis, Univ. Groningen
Ratag, M. A., Pottasch, S. R., Dennefeld, M., & Menzies, J. 1997, A&AS, 126, 297
Richer, M. G. 1993, ApJ, 415, 240
Richer, M. G., & McCall, M. L. 1995, ApJ, 445, 642
Richer, M. G., McCall, M. L., & Stasińska, G. 1998, A&A, 340, 67
Rudolph, A. L., Simpson, J. P., Haas, M. R., Erickson, E. F., & Fich, M. 1997, ApJ, 489, 94
Skillman, E. D. 1989, ApJ, 347, 883
Simpson, J. P., Colgan, S. W. J., Rubin, R. H., Erickson, E. F., & Haas, M. R. 1995, ApJ, 444, 721
Spitzer, L., Jr. 1948, ApJ, 107, 6
Spitzer, L., Jr. 1949, ApJ, 109, 337
Spitzer, L., Jr., & Savedoff, M. P. 1950, ApJ, 111, 593
Stasińska, G. 1978, A&AS, 32, 429
Stasińska, G. 1980, A&A, 85, 359
Stasińska, G. 2001, in The evolution of Galaxies. I. Observational clues, eds. J. M. Vílchez, G. Stasińska & E. Pérez, Ap&SS, 277, 189
Stasińska, G., & Leitherer, C. 1996, ApJS 107, 661
Stasińska, G., Richer, M. G., & McCall, M. L. 1998, A&A, 336, 667
Stasińska, G., & Schaerer, D. 1999, A&A, 351, 72
Stasińska, G., Schaerer, D., & Leitherer, C. 2001, A&A, 370, 1
Tovmassian, G., Stasińska, G., Chavushyan, V. H., Zharikov, S. V., Gutierrez, C., & Prada, F. 2001, A&A, 370, 456

Grażyna Stasińska: DAEC, Observatoire de Meudon, 92195 Meudon, France (grazyna.stasinska@obspm.fr).

Ionized Gaseous Nebulae (Mexico City, 21-24 November 2000)
Editors: William Henney, José Franco, Marco Martos, & Miriam Peña